Beyond Polymaxenolide: Cembrane-Africanane Terpenoids from the Hybrid Soft Coral *Sinularia maxima* × *S. polydactyla*

Haidy N. Kamel,*[,†] Yuanqing Ding,[‡] Xing-Cong Li,[‡] Daneel Ferreira,[†,‡] Frank R. Fronczek,[§] and Marc Slattery*[,†]

Department of Pharmacognosy, School of Pharmacy, The University of Mississippi, Mississippi 38677, National Center for Natural Products Research, Research Institute of Pharmaceutical Sciences, The University of Mississippi, University, Mississippi 38677, and Department of Chemistry, Louisiana State University, Baton Rouge, Louisiana 70803

Received January 26, 2009

The effects of natural hybridization on secondary metabolite production and diversification have only recently been studied in plants and have essentially been overlooked in marine organisms. Chemical investigation of the hybrid soft coral *Sinularia maxima* × *S. polydactyla* resulted in the isolation of five new terpenoids, 7*E*-polymaxenolide (**1**), 7*E*-5-epipolymaxenolide (**2**), and polymaxenolides A−C (**3**−**5**), possessing a cembrane-africanane skeleton. Their structures were established by detailed analysis of NMR and MS data. The contentious issue of defining the absolute configuration at the stereogenic centers of the conformationally mobile cembrane macrocyclic ring was addressed by joint application of electronic circular dichroism and X-ray diffraction analyses.

Hybridization is a ubiquitous feature of many natural populations. Its significance in terrestrial ecosystems was recognized[1] as early as the 1700 to 1800s, when Linnaeus and Mendel suggested that hybridization could lead to new species.[2] More recently, it was shown that hybridization may assist plants in adapting more efficiently to their environment.[3] It was suggested that resistance of hybrid plants to herbivores, pathogens, and parasites is an important component of hybrid survival.[4] Clearly, the production of new secondary metabolites plays an important role in mediating this hybrid resistance, which suggests the possibility of secondary metabolite diversification through hybridization.[5] Investigation of the chemical consequences of hybridization in the plants *Senecio jacobaea* and *S. aquaticus* using metabolomic profiling demonstrated a quantitative differential expression in the hybrid than either parental species.[5] Other studies showed the formation of unique metabolites in plant hybrids.[6] It has been estimated that the frequency of metabolite novelty resulting from hybridization in plant ecosystems is between 5% and 20%.[7] The implications of these data in natural product research are significant. Hybridization represents a new source of novel molecular entities with potential biomedical and research applications.

Hybridization is less well studied in the marine environment than in terrestrial ecosystems. However, it appears to be a widespread phenomenon that has had a significant impact on the evolution of marine organisms.[8] The coexistence of hundreds of coral species that reproduce in mass-spawning events provides a significant opportunity for hybridization among congenerics.[9] Soft corals of the genus *Sinularia* are prolific in shallow-reef fauna of the tropical Indo-Pacific and are recognized as rich sources of terpenoids. We identified a hybrid zone of *Sinularia maxima* × *S. polydactyla* among soft corals on a back reef community in Guam[10] and isolated an unprecedented metabolite, polymaxenolide, linking a cembrane diterpene and an africanane sesquiterpene skeleton.[11] We proposed a new mechanism for the production of novel compounds in hybrids via enzyme-catalyzed combination of the basic skeletons from the two parental species. Continued investigation of the CH_2Cl_2/MeOH extract of the animal has now furnished additional related metabolites, 7*E*-polymaxenolide (**1**), 7*E*-5-epipolymaxenolide (**2**), and polymaxenolides A−C (**3**−**5**). The structures and absolute configurations were determined on the basis of detailed NMR and MS data analyses, experimental and theoretically calculated electronic circular dichroism (ECD), and X-ray crystallographic analysis.

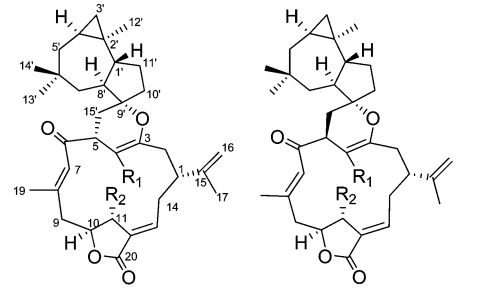

1
R_1= $^{18}COO^{21}CH_3$ R_2= $^{22}OCO^{23}CH_3$

2 R_1= $COOCH_3$ R_2= $OCOCH_3$
3 R_1= $COOCH_3$ R_2= OH

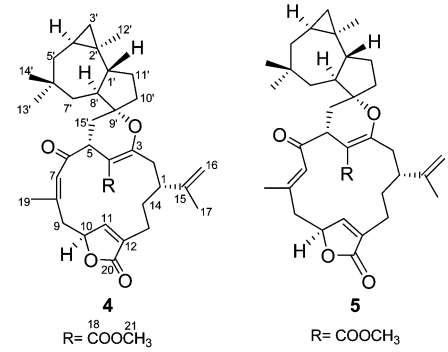

4
R= $^{18}COO^{21}CH_3$

5
R= $COOCH_3$

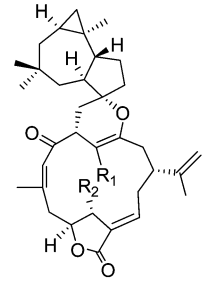

6 polymaxenolide
R_1= $COOCH_3$ R_2=$OCOCH_3$

* To whom correspondence should be addressed. Tel: +1-662-915-1706. Fax: +1-662-915-6975. E-mail: hnkamel@olemiss.edu. Tel: +1-662-915-1053. E-mail: slattery@olemiss.edu.
† Department of Pharmacognosy, University of Mississippi.
‡ National Center for Natural Product Research, University of Mississippi.
§ Louisiana State University.

10.1021/np900040w CCC: $40.75
Published on Web 04/03/2009

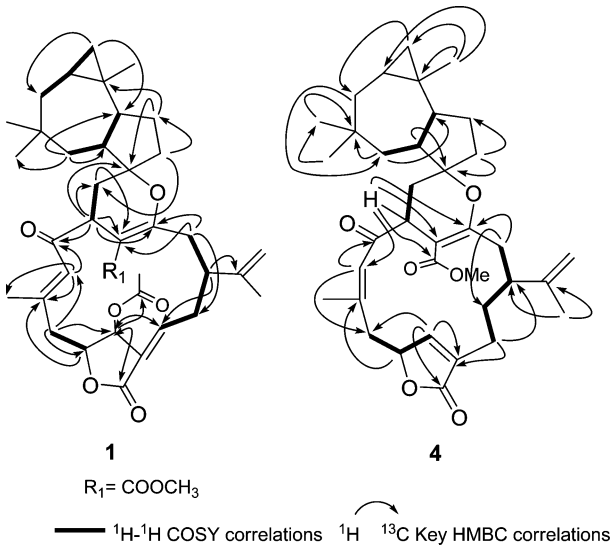

Figure 1. HMBC and COSY correlations of compounds **1** and **4**.

Results and Discussion

Preliminary ^{1}H NMR analyses of compounds **1**−**5** revealed structural similarity and indicated the presence of a common cembrane-africanane linked skeleton. The HRESIMS of compound **1** exhibited a molecular ion peak at *m/z* 657.3922 ([M + Na]$^+$). When considered in conjunction with ^{1}H and ^{13}C NMR data, this suggested a molecular formula of $C_{38}H_{50}O_8$ with 14 degrees of unsaturation. A carbonyl absorption in the IR spectrum at 1692 cm^{-1}, together with the carbon resonance at δ_C 200.0, reflected the presence of a β,β-disubstituted α,β-unsaturated ketone moiety. This was further supported by HMBC correlations between the olefinic proton at δ 6.02 and the carbon resonances at δ_C 200.0 (C-6, q), 152.2 (C-8, q), and 45.4 (C-9, CH_2) and a vinylic methyl at δ_C 19.2 (C-19, CH_3). Three additional carbonyl carbons were deduced from absorptions in the IR spectrum at 1715, 1739, and 1764 cm^{-1}. Proton resonances at δ 7.25 and 5.59 and carbon resonances at δ_C 152.2, 125.7, 78.7, and 75.4 suggested the presence of an exocyclic α,β-unsaturated γ-lactone functionality and accounted for the IR absorption at 1764 cm^{-1}. A proton resonance at δ 3.49 (3H, s) that was correlated in the HMBC spectrum with a carbonyl carbon at δ_C 166.9 indicated the presence of an α,β-unsaturated methyl ester functionality residing at C-4. Further examination of the NMR data showed the presence of an isopropenyl group [δ 4.92 (1H, s); 4.94 (1H, s) and 1.87 (3H, s)] at C-1 on the basis of the HMBC correlations between H-1 and H_3-17 and H_2-16. These partial structures were connected by analysis of the 2D NMR data. The key HMBC correlations are shown by solid arrows in Figure 1. The presence of the 14-membered carbocylic cembranoid ring was disclosed by HMBC correlations (H-10 to C-8, H-9 to C-7 and C-10, H-13 to C-1 and C-12, H-2 to C-3, C-4, and C-14, and H-5 to C-3 and C-4) and from connections of the different proton spin systems of the cembrane skeleton through ^{1}H−^{1}H COSY correlations (Figure 1). Additionally, the ^{1}H NMR spectrum showed resonances attributable to a trisubstituted cyclopropyl ring [δ 0.13 (1H, t), 0.39 (1H, m), and 0.51 (1H, dd)] and three additional tertiary methyl carbons [δ 0.94 (3H, s), 0.98 (3H, s), and 1.10 (3H, s)]. HMBC correlations starting from the cyclopropyl methylene protons and downward, as shown in Figure 1, assembled the northern part of the molecule, which is connected to the 14-membered cembrane ring via a dihydropyrano moiety, the dihydropyranyl and cyclopentyl rings being joined via spiro carbon C-9′.

At this stage, it was evident that compound **1** has the same planar structure as polymaxenolide (**6**).[11] The significant upfield shift observed for C-19 ($\Delta\delta_C$ −8.2 ppm) and the downfield shift of C-9 ($\Delta\delta_C$ +10.5 ppm) in comparison with those of **6** suggested that compound **1** is the $\Delta^{7(8)}$ geometrical isomer of polymaxenolide (**6**). According to the NOESY spectrum, H-7 did not correlate with H_3-19, confirming the *E*-geometry of the 7,8-double bond. Thus, compound **1** was identified as 7*E*-polymaxenolide.

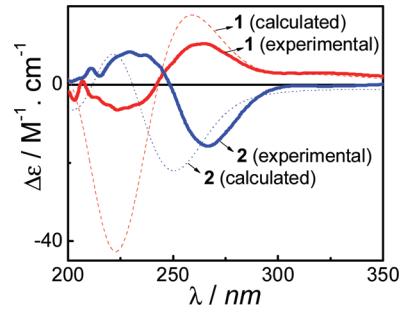

Figure 2. Calculated and experimental ECD of compounds **1** and **2**.

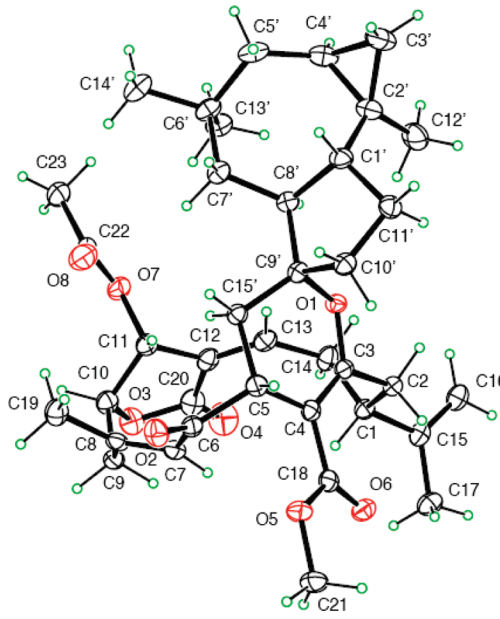

Figure 3. ORTEP plot of compound **1** showing the atomic numbering and the absolute configuration.

Further analysis of the NOESY spectrum showed correlations between H-4′/H_3-12′, H_3-12′/H_3-13′, H-3′/H-8′, and H-8′/H-7′α, which indicated that these protons/methyl groups are cofacial. An NOE correlation observed between H-11 and H-13 established the *Z*-configuration of the 12,13-double bond, while the NOE association between H-13 and H-14α and between H-14β and H-1 indicated the α-orientation of the isopropenyl group.

On the basis of an X-ray crystallographic analysis, the structure of polymaxenolide (**6**) was recently published as the enantiomer of the compound shown here.[11] Initial X-ray crystallographic data similarly defined the structure of 7*E*-polymaxenolide (**1**) as enantiomeric to the configuration depicted in **1**. Thus, we took recourse to electronic circular dichroism (ECD) in order to define the absolute configuration of compound **1** unambiguously.

The ECD spectrum of compound **1** (Figure 2) shows sequential positive and negative Cotton effects (CE) at 265 and 223 nm, respectively. A UV absorption maximum at ca. 240 nm confirms that the observed CEs are indicative of exciton coupling[12] arising from the exocyclic α,β-unsaturated lactone and α,β-unsaturated ketone chromophores. From Dreiding models and the energy-minimized molecular model of compound **1** (Figure 4), it is evident that the electronic transition dipole moments of these chromophores,

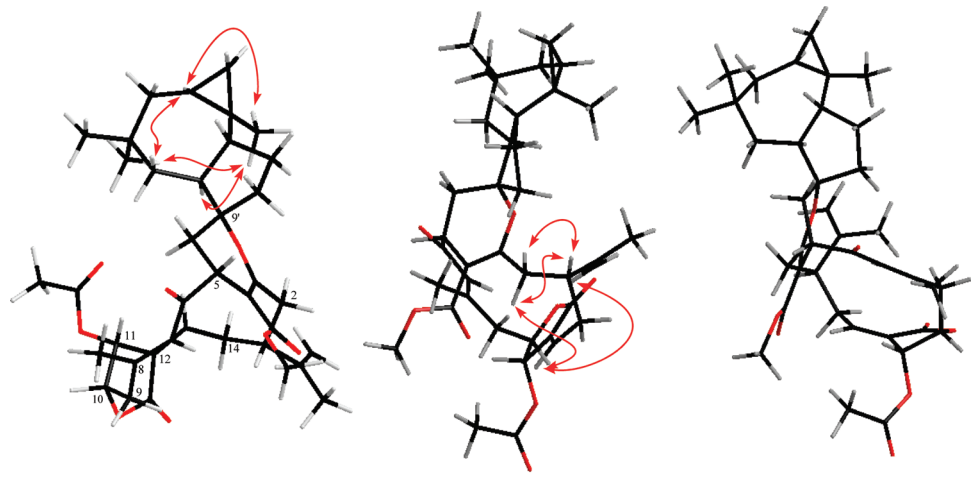

Figure 4. Energy-minimized molecular model of **1**, **2**, and **2′** with diagnostic NOESY correlations observed.

Table 1. ^{13}C NMR Data for Compounds **1**−**5**

carbon	**1**[a]	**2**[a]	**3**[a]	**4**[a]	**5**[b]
1	48.9	40.1	40.0	46.2	46.7
2	42.2	32.3	32.2	40.7	40.5
3	170.9	166.9	167.0	171.2	171.1
4	102.7	101.1	100.7	100.5	101.6
5	47.1	44.7	44.7	46.9	46.4
6	200.0	201.2	200.9	200.8	200.9
7	124.3	125.1	124.6	122.1	125.9
8	152.2	151.3	151.8	150.1	149.0
9	45.4	41.8	41.8	39.8	45.8
10	78.7	82.1	83.9	77.8	77.7
11	75.4	75.2	73.0	148.0	146.3
12	125.7	124.7	129.9	135.4	135.7
13	152.2	152.6	149.1	22.6	22.3
14	30.9	29.5	29.2	28.8	27.8
15	150.0	147.8	148.0	147.7	147.1
16	110.4	110.9	110.8	112.5	112.9
17	20.8	22.4	22.5	19.8	19.8
18	166.9	169.1	168.8	167.2	167.3
19	19.2	22.6	22.3	22.1	19.2
20	167.0	167.9	168.8	173.2	172.6
21	51.3	51.5	51.0	51.0	51.3
22	170.2	170.9			
23	21.3	20.5			
1′	50.6	51.4	51.8	49.7	49.1
2′	20.1	20.1	20.0	20.4	20.6
3′	24.7	23.6	23.5	24.0	24.0
4′	22.5	22.1	22.0	22.5	22.3
5′	43.6	43.4	43.3	43.8	43.5
6′	33.9	33.8	33.6	33.9	33.8
7′	45.0	45.5	45.4	44.0	45.5
8′	47.7	48.2	48.1	47.9	47.7
9′	89.1	88.9	88.8	88.6	88.0
10′	35.4	38.8	38.9	35.8	35.2
11′	23.8	25.5	25.3	24.4	24.2
12′	20.2	20.0	19.9	20.0	20.0
13′	24.3	24.5	24.4	24.4	24.5
14′	34.3	34.4	34.2	34.4	34.5
15′	34.9	28.4	28.4	30.1	30.4

[a] Data recorded in C_6D_6 at 150 MHz. [b] Data recorded in C_6D_6 at 100 MHz.

aligning C-13−C-20 and C-6−C-8, constitutes positive exciton chirality and strongly indicates a 10*S* absolute configuration.

Theoretical calculations of ECD spectra have been demonstrated as a powerful tool for defining the absolute configuration of natural products.[13−15] Thus, ECD calculations using TDDFT at the B3LYP-SCRF/6-31G**//B3LYP/6-31G** level were carried out on compound **1** and its enantiomer. The experimental and calculated ECD spectra of **1** and the calculated ECD spectrum of *ent*-**1** were virtually opposites. However, the calculated ECD spectrum of compound **1** closely matched the experimental spectrum of **1** (Figure 2). The calculated positive and negative CEs at 255 and 224 nm, respectively, correspond with the experimental CEs at 265 and 223 nm, respectively. The larger amplitude of the short-wavelength CE near 220 nm in the calculated ECD spectrum presumably results from minor conformational differences between the calculated and solution conformers. The natural product (**1**) was accordingly assigned as 1*R*, 5*R*, 10*S*, 11*R*, 1′*R*, 2′*R*, 4′*S*, 8′*S*, 9′*R*-7*E*-polymaxenolide.

The assigned absolute configuration of 7*E*-polymaxenolide (**1**) was confirmed by refinement of the structure using low-temperature (90 K) X-ray diffraction data from a Bruker Kappa Apex-II diffractometer equipped with Cu Kα radiation and was based on resonant scattering of the light atoms only, principally oxygen. Refinement of the Flack parameter[16] led to a value of $X = 0.03(13)$. Analysis of 1904 Bijvoet pairs using the method of Hooft et al.[17] yielded $Y = -0.04(4)$, corresponding to a probability of 1.000 that the reported absolute configuration is correct. An ORTEP plot of compound **1** is shown in Figure 3.

It should be emphasized that the definition of both relative and absolute configuration of macrocylic ring systems like those in the cembranolides is not trivial. Owing to the conformational mobility of these ring systems, stereochemical information drawn from through-space ^{1}H NMR data is less reliable than for more rigid rings, often leading to ambiguous conclusions. Thus, we were extremely pleased with the configurational conclusions emanating from a combination of the two most powerful methods for stereochemical assignment, i.e., circular dichroism and X-ray diffraction crystallography.

Compound **2** was obtained as an amorphous solid. On the basis of its HRESIMS (*m*/*z* 657.3271, $[M + Na]^+$) along with the ^{1}H and ^{13}C NMR data, the molecular formula was established as $C_{38}H_{50}O_8$. As in the case of **1**, the physical data of **2** also revealed the presence of β,β-disubstituted α,β-unsaturated ketone (IR ν_{max} 1693 cm^{-1}, δ_C 201.2, 151.3, 125.1), α,β-conjugated methyl ester (IR ν_{max} 1713 cm^{-1}, ^{13}C NMR δ 51.3, 166.9), and exocyclic α,β-unsaturated γ-lactone (IR ν_{max} 1761 cm^{-1}, δ_C 75.4, 125.7, 167.0, 78.7) functionalities. The ^{1}H NMR data showed resonances attributed to an isopropenyl group (δ_H 4.82, 5.01, 1.55) and a trisubstituted cyclopropyl ring (δ_H 0.09, 0.36, 0.48).

Analysis of the 2D NMR data provided evidence for the gross structure of **2**, which was the same as that of **1**. Thus, **2** was believed to be a stereoisomer of **1**. Compound **2** exhibited significant upfield shifts at C-1, C-2, C-3, C-5, and C-15′, suggesting a configurational change at C-1 and/or C-5 as compared to the structure of **1**.

Table 2. ^{1}H NMR Data for Compounds **1**−**5**

	1[a]	**2**[a]	**3**[a]	**4**[a]	**5**[b]
H	δ (mult, J in Hz)	δ (mult, J in Hz)	δ (mult, J in Hz)	δ (mult, J in Hz)	δ (mult, J in Hz)
1	2.91, brt (16)	2.95, brt (5.4)	2.92, brt (6)	2.72, brt (11.5)	2.54, brt (11.5)
2	2.10, brd (19)	2.22, brdd (14, 5.4)	2.22, brdd (14.5, 6)	1.95, t (12)	1.89, t (12)
	3.79, d (19)	4.48, brd (14)	4.47, d (14.5)	3.65, brd (12)	3.79, brd (12)
3					
4					
5	3.53, brd (8)	3.59, brd (3)	3.53, m	3.56, dd (12.2, 6.8)	3.59, dd (12, 7)
6					
7	6.02, brs	6.05, brs	5.76, brs	5.77, brs	5.96, brs
8					
9	1.80, m	2.36, dd (16, 6)	1.80, brd (16)	1.82, m	1.50, m
	2.28, m	2.60, d (16)	2.17, dd (16, 6)	2.04, m	2.29, m
10	4.22, t (12)	4.22, d (6)	4.19, d (6)	4.18, brd (7.5)	4.26, brt (5.4)
11	5.59, brs	5.71, brs	4.43, s	6.40, s	6.83, s
12					
13	7.25, dd (17, 8.5)	7.56, d (8)	7.22, d (8.5)	2.04, m	2.06, m
				2.50, dd (16, 7)	2.60, dd (18, 12)
14	1.73, m	2.76, brd (20)	2.66, brd (18)	1.76, m	1.67, m
	4.05, t (18)	3.82, dt (20, 8)	3.76, dt (18, 6)	1.98, m	2.02, m
15					
16	4.92, brs	4.82, brs	4.82, brs	4.96, brs	4.89, brs
	4.94, brs	5.01, brs	4.99, brs	5.01, brs	4.95, brs
17	1.87, s	1.55, s	1.56, s	1.69, s	1.66, s
18					
19	1.99, s	2.14, s	2.04, s	2.04, s	1.76, s
20					
21	3.40, s	3.45, s	3.29, s	3.38, s	3.38, s
22					
23	1.60, s	1.47, s			
1′	0.82, m	0.91, m	0.89, m	0.93, m	0.93, m
2′					
3′	0.15, t (6.6)	0.09, t (4.2)	0.03, t (4)	0.13, t (4.2)	0.14, t (4.2)
	0.55, dd (12, 6.6)	0.48, dd (8.6, 4.2)	0.43, dd (8.4, 4)	0.51, dd (7.5, 4.2)	0.53, dd (7.8, 4.2)
4′	0.44, m	0.36, m	0.30, m	0.39, m	0.38, m
5′	0.87, m	0.88 L, m	0.81, m	0.89, dd (14, 10.8)	0.85, dd (14.4, 10.8)
	1.76, m	1.68, brd (6)	1.62, dd (14, 6)	1.76, m	1.68, m
6′					
7′	0.74, t (18)	0.73, t (12.6)	0.66, t (12.5)	0.74, t (12.6)	0.74, t (12.6)
	1.51, m	1.44, m	1.40, bd (12.5)	1.76, m	1.40, m
8′	2.30, m	2.10, m	2.06, m	2.32, brt (10)	2.27, m
9′					
10′	1.22, m	1.31, m	1.26, m	1.25, m	1.26, m
	1.55, m	1.76, m	1.73, m	1.54, m	1.53, m
11′	1.13, m	1.67, m	1.54, m	1.25, m	1.55, m
	1.55, m	1.76, m	1.76 (m	1.58, m	1.67, m
12′	0.98, s	0.96, s	0.90, s	0.93, s	0.93, s
13′	1.10, s	0.90, s	0.88, s	1.18, s	1.00, s
14′	0.94, s	0.84, s	0.78, s	1.10, s	0.82, s
15′	1.29, m	1.44, m	1.43, dd (13, 7.2)	1.53, m	1.39, m
	2.04, brd (8)	2.46, dd (13, 3)	2.38, d (13)	1.65, m	1.69, m

[a] Data recorded in C_6D_6 at 600 MHz. [b] Data recorded in C_6D_6 at 400 MHz.

Calculated ECD spectra defined two (**2**, **2′**) of the three possible structures in which the calculated spectra conform with the experimentally observed CEs. Distinction between these two structures was achieved by a combination of NOESY and simple molecular modeling studies. Key NOE correlations are shown in Figure 4. It is evident that the observed correlations are consistent with structure **2** only. Thus, a NOESY correlation between H-13 and H_3-17 is possible in structure **2**. Reversing the configuration at C-5 results in significant conformational change, as evidenced in Figure 4. In such a conformation, the allylic H-2α lies close to the carbonyl group of the lactone ring and, therefore, is in the deshielding zone of the induced magnetic field, to explain its downfield shift at δ 4.48. The profound effect of the conformational change of the cembranoid ring on the ECD spectrum of compound **2** (7*E*-5-epipolymaxenolide) is demonstrated in Figure 2. Superficially, the calculated and experimental spectra of compounds **1** and **2** may be interpreted such that these compounds are indeed enantiomers. However, comparison of the minimum energy conformers of **1** and **2** indicates the dramatic conformational changes and, hence, vastly different chiroptical properties resulting from inversion of configuration at C-5. Dreiding models and the energy-minimized molecular model of **2** (Figure 4) clearly indicate that inversion of configuration at C-5 realigns the electronic transition dipole moments of the exocyclic α,β-unsaturated lactone and ketone chromophores to now reflect negative exciton chirality and hence 5*S*- as opposed to 5*R*-configuration in compound **1**.

Polymaxenolide A (**3**) was obtained as a colorless oil. Its HRESIMS and the ^{1}H and ^{13}C NMR data suggested a molecular formula of $C_{36}H_{48}O_7$, consistent with 13 degrees of unsaturation. In contrast to compounds **1** and **2**, a hydroxy group was suggested to be present in **3** ($IR_{\nu max}$ 3418). The ^{13}C NMR spectrum displayed 36 carbon resonances that were similar to compound **2** except for the absence of the resonances attributed to the C-11 *O*-acetyl functionality in **2** (δ_C 170.9, 20.5). Additionally, the ^{1}H NMR spectrum showed H-11 shifted at δ 4.43, confirming the presence of a hydroxy group at C-11. The similar ^{13}C NMR chemical shift values shown by both compounds **2** and **3** for C-1, C-2, C-5, C-10, C-11, C-1′, C-2′, C-4′, C-6′, C-8′, and C-15′ suggested the same configuration at these sites. Analysis of NOESY correlations along

with ECD calculations (Supporting Information) confirmed the absolute configuration as shown.

Polymaxenolide B (**4**), an amorphous solid, had a molecular formula of $C_{36}H_{48}O_6$ by HRESIMS {$[M + H]^+$ at *m*/*z* 577.3346}, indicating 13 degrees of unsaturation. The ^1H and ^{13}C NMR spectra were similar to those of **3**. Indeed, the IR and NMR spectra of **3** confirmed the presence of africanane (δ_H 0.13, 0.39, 0.51), β,β-disubstituted-α,β-unsaturated ketone, and α,β-unsaturated methyl ester moieties and the absence of acetate functionalities. Additionally, the ^{13}C NMR spectrum showed only one oxymethine carbon at δ_C 77.8 and an additional methylene carbon at δ_C 22.6 when compared with the data of **1**. These data along with the ^{13}C NMR resonances at δ_C 135.4 and 148.0 suggested that compound **4** possessed an endocylic α,β-unsaturated γ-lactone moiety. Thus, **4** is presumably related to **3** via a process equivalent to reductive dehydration. HMBC and COSY correlations confirmed the structure of **4** as shown in Figure 1. The *Z*-geometry of the Δ^7 double bond in **4** was supported by a strong NOE correlation between H-7 and Me-19. NOESY correlations indicated that compound **4** possessed the same relative configuration as compound **1** at C-1′, C-2′, C-4′, C-7′, C-8′, C-9′, and C-5. The absolute configuration of compound **4** (1*R*, 5*R*, 10*S*, 1′*R*, 2′*R*, 4′*S*, 8′*S*, 9′*R*) was then determined based on ECD calculations.

The molecular formula of **5** ($C_{36}H_{48}O_6$) was identical to that of **4**, as determined by HRESIMS {$[M + Na]^+$ 599.3227}, indicating the isomeric nature of these compounds. Furthermore, the ^1H and ^{13}C NMR data were similar to those of **4**, and using 2D NMR data, **5** was shown to possess the same molecular framework as **4**. However, the upfield shift observed for C-19 ($\Delta\delta_C$ −2.9 ppm) and the downfield shift of C-7 ($\Delta\delta_C$ +3.8 ppm) and C-9 ($\Delta\delta_C$ +7.0 ppm) in comparison with those of **4** suggested that **5** possessed a different geometry for the 7,8 double bond. According to the NOESY spectrum of **5**, H-7 did not show NOE correlation with H_3-19, confirming the *E*-geometry of the 7,8-double bond. The configurations at the remaining stereogenic centers are similar to those of **4** on the basis of the NOE correlations. An excellent match of the calculated and experimental ECD spectra (Supporting Information, Figure S6) finally confirmed the absolute configuration of **5** as shown.

We recently interpreted CEs similar to those in Figure 2, shown by diterpene furanocembranolides,[18] in terms of an empirical CD rule formulated to define the absolute configuration of 5-substituted 2(5*H*)-furanones,[19] a functional group also present in compounds **4** and **5**. Thus, the high-amplitude positive and negative CEs for the $n \rightarrow \pi^*$ and $\pi \rightarrow \pi^*$ transitions near 260 and 220 nm, respectively, were interpreted as indicative of a 10*R*-configuration. Inversed CEs in the 260 and 220 nm regions of the CD spectra of a series of furanocembranolides from *Leptogorgia alba*[20] were similarly reconciled with the 10*S*-configuration.

The sequential negative and positive CEs in the CD spectra of the pukalide derivatives[20] were also interpreted in terms of the nonempirical exciton chirality method.[12] Thus, when the electronic transition dipole moments of the α,β-unsaturated lactone and ketone chromophores are aligned to subtend negative exciton chirality, it indicates an 8*R*-configuration for the pukalide derivatives (equivalent to position 10 in our compounds **1**−**5**). Conversely, the observed positive exciton chirality in the CD spectrum of compounds **4** and **5**, and the analogous compounds published earlier,[19] is then in accordance with the *R* absolute configuration at C-10. Application of both the empirical and nonempirical CD rules hence gives the correct absolute configuration at C-10 of compounds **4**, **5**, and their analogues[19] and at C-8 of the pukalide derivatives.[20]

It should be emphasized that the ECD calculations were based on the X-ray crystal structure of compound **1**, which provided a good starting conformation despite the fact that it may not accurately reflect the solution conformation. This also provided the foundation for conformational optimization of compounds **2**−**5**. We did not perform an extensive conformational search for these conformationally flexible molecules due to the excessive computational time that would be necessitated by such an approach. However, our calculations afforded ECD spectra that closely matched the experimental data. We are thus confident in the configuration conclusions regarding compounds **1**−**5**.

The structures of polymaxenolide and related compounds (**1**−**5**), comprising a 14-membered cembranoid ring and an africanane skeleton linked via a spiro ring system, are native to the hybrid *Sinularia maxima* × *S. polydactyla*. It has been argued earlier that distinct secondary metabolites result from novel merging of two separate biosynthetic pathways.[21] Thus, their production may require only a single enzyme capable of connecting the products from two different pathways. Alternatively, new metabolites may be produced by unique extensions of existing pathways. Ongoing studies in our laboratory are directed toward the understanding of the biosynthesis of these unusual metabolites.

Experimental Section

General Experimental Procedures. Optical rotations were measured with a JASCO DIP-370 digital polarimeter. CD spectra were recorded on a JASCO J-715 spectropolarimeter. UV spectra were recorded on a Hewlett-Packard 8452A diode array spectrometer. IR spectra were recorded on an ATI Mattson Genesis series FTIR spectrometer. NMR spectra were measured on Bruker Advance DRX-400 and DRX-600 spectrometers. ^1H and ^{13}C NMR spectra were measured and reported in ppm by using the benzene-d_6 solvent peak (δ_H 7.16 and δ_C 128.3) as an internal standard. ESI-FTMS analyses were measured on a Bruker-Magnex BioAPEX 30es ion cyclotron HR HPLC-FT spectrometer by direct injection into an electrospray interface. HPLC was carried out on a Waters 2695 model system (Phenomenex Ultracarbon, C18, 5 μm, 250 × 10 mm; flow rate, 2 mL/min; detector wavelength, 254 nm). Theoretical ECD calculations were performed at 298 K by the Gaussian03 program package.[22] Ground-state geometries were optimized at the B3LYP/6-31G** level, total energies of individual conformers were obtained, and vibrational analysis was done to confirm these minima. The "self-consistent reaction field" method (SCRF) with the "conductor-like continuum solvent model" (COSMO) was employed to perform the ECD calculation in methanol solution at the B3LYP-SCRF/6-31G**//B3LYP/6-31G** level.[15,23–25]

Animal Material. The hybrid soft coral *Sinularia maxima* × *S. polydactyla* was collected at Piti Bomb holes, a shallow reef on the Leeward side of Guam (13°25′ N, 144°55′ E). A voucher specimen of the coral (GU30503093) was deposited at the NOAA Ocean Biotechnology Center and Repository, Oxford, MS.

Extraction and Isolation. The frozen soft coral was exhaustively extracted with 1:1 MeOH−CH_2Cl_2, and the combined solvent extracts were concentrated under reduced pressure. The extract (28 g) was subjected to Si gel vacuum liquid chromatography (VLC) eluted with hexanes, hexanes−EtOAc, EtOAc−MeOH, and MeOH to yield 11 fractions. The fraction (4 g) eluted with 8:2 hexanes−EtOAc was purified by Si gel VLC using gradient elution of EtOAc−hexanes to afford 18 fractions (I−XIII). Purification of fraction VIII (430 mg) on Si gel VLC using a step gradient of EtOAc−hexanes as eluent yielded 10 fractions. The sixth fraction (114 mg) was purified on HPLC using an isocratic elution with 5:95 H_2O−MeOH to yield compounds **2** (7 mg), **3** (6 mg), and **4** (5 mg), while the seventh (27 mg) and the eighth (49 mg) fractions were purified on RP HPLC using an isocratic elution with 1:9 water−MeOH to yield compounds **1** (10 mg) and **5** (1 mg), respectively.

Single-Crystal X-ray Diffraction Analysis of Compound 1. Crystallization of compound **1** by slow evaporation from MeOH yielded colorless crystals. Diffraction data for **1** were collected to $\theta_{max} = 30.8°$ at $T = 90$ K on a Nonius KappaCCD diffractometer equipped with Mo Kα radiation and an Oxford Cryostream sample chiller. Refinement to $R = 0.043$ established the identity of **1**, but left open the issue of absolute configuration. In order to establish the absolute configuration crystallographically, a data set was collected to $\theta_{max} = 68.9°$ at $T = 90$ K on a Bruker KappaApex-II diffractometer equipped with Cu Kα radiation, yielding 1622 Bijvoet pairs. Refinement of the structure yielded $R = 0.031$, and refinement of the Flack parameter[16] yielded a value of 0.03(13). Interpretation of the Bijvoet pairs by the Bayesian statistical method of Hooft et al.[17] as implemented in PLATON[26]

yielded a Hooft parameter of −0.04(4), corresponding to a probability of 1.000 that the configuration shown in Figure 2 is correct.

Compound 1: colorless crystals (MeOH); mp 120−127 °C; $[\alpha]^{25}_{D}$ +37.8 (*c* 0.14, MeOH); UV (MeOH) λ_{max} (log ϵ) 200 (3.67) nm, 236 (3.73) nm; CD (*c* 3.16 × 10^{-4} M, MeOH) λ ($\Delta\epsilon$) 265 (10.5), 223 (−6.5); IR (NaCl) ν_{max} 2950, 2360, 1764, 1712, 1692, 1599, 1435, 1367, 1266, 1255, 1089, 755 cm^{-1}; ^{1}H NMR (C_6D_6, 600 MHz) see Table 2; ^{13}C NMR (C_6D_6, 100 MHz) see Table 1; HRESIMS *m/z* 657.3922 $[M + Na]^+$ (calcd for $C_{38}H_{50}O_8Na$, 657.3403).

Compound 2: amorphous solid; $[\alpha]^{25}_{D}$ −13.3 (*c* 0.105, MeOH); UV (MeOH) λ_{max} (log ϵ) 201 (3.72) nm, 235 (3.55) nm; CD (*c* 3.16 × 10^{-4} M, MeOH) λ ($\Delta\epsilon$) 267 (−16.3), 229 (8.4); IR (NaCl) ν_{max} 2949, 2349, 1761, 1702, 1693, 1598, 1436, 1228, 1075, 897, 756 cm^{-1}; ^{1}H NMR (C_6D_6, 600 MHz) see Table 2; ^{13}C NMR (C_6D_6, 100 MHz) see Table 1; HRESIMS *m/z* 657.3271 $[M + Na]^+$ (calcd for $C_{38}H_{50}O_8Na$, 657.3403).

Compound 3: colorless oil; $[\alpha]^{25}_{D}$ +45.3 (*c* 0.13, MeOH); UV (MeOH) λ_{max} (log ϵ) 201 (3.98) nm, 238 (3.95) nm; CD (*c* 3.38 × 10^{-4} M, MeOH) λ ($\Delta\epsilon$) 267 (−36.9); IR (NaCl) ν_{max} 3418, 2924, 1752, 1702, 1680, 1598, 1437, 1296, 896 cm^{-1}; ^{1}H NMR (C_6D_6, 600 MHz) see Table 2; ^{13}C NMR (C_6D_6, 100 MHz) see Table 1; HRESIMS *m/z* 615.3297 $[M + Na]^+$ (calcd for $C_{36}H_{48}O_7Na$, 615.3369).

Compound 4: colorless oil; UV (MeOH) λ_{max} (log ϵ) 202 (4.25) nm, 234 (4.24) nm; CD (*c* 3.47 × 10^{-4} M, MeOH) λ ($\Delta\epsilon$) 319 (3.1), 261 (10.1), 238 (−23.9); IR (NaCl) ν_{max} 2901, 1761, 1707, 1686, 1560, 1411, 1244, 802 cm^{-1}; ^{1}H NMR (C_6D_6, 400 MHz) see Table 2; ^{13}C NMR (C_6D_6, 75 MHz) see Table 1; HRESIMS *m/z* 615.3297 $[M + Na]^+$ (calcd for $C_{36}H_{48}O_7Na$, 615.3369).

Compound 5: colorless oil; $[\alpha]^{25}_{D}$ +22.7 (*c* 0.11, MeOH); UV (MeOH) λ_{max} (log ϵ) 202 (4.14) nm, 240 (3.89) nm; CD (*c* 1.74 × 10^{-4} M, MeOH) λ ($\Delta\epsilon$) 255 (30.7), 210 (−19.2); IR (NaCl) ν_{max} 2901, 1761, 1707, 1686, 1560, 1411, 1224, 1100, 1092, 802, 757 cm^{-1}; ^{1}H NMR (C_6D_6, 600 MHz) see Table 2; ^{13}C NMR (C_6D_6, 100 MHz) see Table 1; HRESIMS *m/z* 599.3227 $[M + Na]^+$ (calcd for $C_{36}H_{48}O_6Na$, 599.3348).

CCDC 677353 (compound **1**, Mo data) and 677354 (compound **1**, Cu data) contain the supplementary crystallographic data for this paper. These data can be obtained free of charge at www.ccdc.cam.ac.uk/conts/retrieving.html [or from the Cambridge Crystallographic Data Centre (CCDC), 12 Union Road, Cambridge CB2 1EZ, UK; fax: +44(0)1223-336033; email: deposit@ccdc.cam.ac.uk].

Acknowledgment. This work was supported in part by the United States Department of Agriculture, Agricultural Research Service Specific Cooperative Agreement No. 58-6048-0009, and the National Oceanic and Atmospheric Association's National Undersea Research Program (NOAA NIUST NA16RU1496).

Supporting Information Available: NMR spectra and calculated ECD data for compounds **1**−**5** and crystallographic information files for compound **1**. This material is available free of charge via the Internet at http://pubs.acs.org.

References and Notes

(1) Rieseberg, L. H.; Carney, S. E. *New Phytol.* **1998**, *140*, 559–624.
(2) Arnold, M. L. In *Natural Hybridization and Evolution*; Oxford University Press: Oxford, UK, XXXX.
(3) Fritz, R. S.; Nicholas-Orians, C. M.; Brunsfeld, S. J. *Oecologia* **1994**, *97*, 106–117.
(4) Fritz, R. S.; Moulia, C.; Newcombe, G. *Ann. Rev. Ecol. Evol. Syst.* **1999**, *30*, 565–591.
(5) Kirk, H.; Choi, Y. H.; Kim, H. K.; Verpoorte, R.; Meijden, E. *New Phytol.* **2005**, *167*, 613–622.
(6) (a) Levy, M.; Levin, D. A. *Am. J. Bot.* **1974**, *61*, 156–167. (b) Crins, W. J.; Bohm, B. A.; Carr, G. D. *Syst. Bot.* **1988**, *3*, 567–571. (c) Buschmann, H.; Spring, O. *Phytochemistry* **1994**, *39*, 367–371.
(7) Orians, C. M. *Am. J. Bot.* **2000**, *87*, 1749–1756.
(8) Willis, B. L.; van Oppen, M. J. H.; Miller, D. J.; Vollmer, S. V.; Ayre, D. J. *Ann. Rev. Ecol. Evol. Syst.* **2006**, *37*, 489–517.
(9) Veron, J. E. N. *Corals in Space and Time: The Biogeography and Evolution of Scleractinia*; Cornell University Press, Ithaca, NY, 1995.
(10) Slattery, M.; Kamel, H. N.; Ankisetty, S.; Gochfeld, D. J.; Hoover, C. A.; Thacker, R. W. *Ecol. Monogr.* **2008**, *78*, 423–443.
(11) Kamel, H. N.; Fronczek, F. R.; Fischer, N. H.; Slattery, M. *Tetrahedron Lett.* **2004**, *45*, 1995–1997.
(12) Berova, N.; Nakanishi, K. In *Circular Dichroism Principles and Applications*; Berova, N., Nakanishi, K., Woody, R. W., Eds.; John Wiley & Sons: New York, 2000; Chapter 12, pp 337−382.
(13) Diedrich, C.; Grimme, S. *J. Phys. Chem. A* **2003**, *107*, 2524–2539.
(14) Stephens, P. J.; McCann, D. M.; Butkus, E.; Stončius, S.; Cheeseman, J. R.; Frisch, M. J. *J. Org. Chem.* **2004**, *69*, 1948–1958.
(15) Ding, Y.; Li, X.-C.; Ferreira, D. *J. Org. Chem.* **2007**, *72*, 9010–9017.
(16) Flack, H. D. *Acta Crystallogr.* **1983**, *A39*, 876–881.
(17) Hooft, R W. W.; Straver, L. H.; Spek, A. L. *J. Appl. Crystallogr.* **2008**, *41*, 96–103.
(18) Kamel, H. N.; Ferreira, D.; Garcia-Fernandez, L. F.; Slattery, M. *J. Nat. Prod.* **2007**, *70*, 1223–1228.
(19) Gawronski, J. K.; Van Oeveren, A.; Van der Deen, H.; Leung, C. W.; Feringa, B. L. *J. Org. Chem.* **1996**, *61*, 1513–1515.
(20) Gutiérrez, M.; Capson, T. L.; Guzmán, H. M.; González, J.; Ortega-Barría, E.; Quiñoá, E.; Riguera, R. *J. Nat. Prod.* **2005**, *68*, 614–616.
(21) McKey, D. *Am. Naturalist* **1980**, *115*, 754–759.
(22) Frisch, M. J.; Trucks, G. W.; Schlegel, H. B.; Scuseria, G. E.; Robb, M. A.; Cheeseman, J. R.; Montgomery, J. A., Jr.; Vreven, T.; Kudin, K. N.; Burant, J. C.; Millam, J. M.; Iyengar, S. S.; Tomasi, J.; Barone, V.; Mennucci, B.; Cossi, M.; Scalmani, G.; Rega, N.; Petersson, G. A.; Nakatsuji, H.; Hada, M.; Ehara, M.; Toyota, K.; Fukuda, R.; Hasegawa, J.; Ishida, M.; Nakajima, T.; Honda, Y.; Kitao, O.; Nakai, H.; Klene, M.; Li, X.; Knox, J. E.; Hratchian, H. P.; Cross, J. B.; Adamo, C.; Jaramillo, J.; Gomperts, R.; Stratmann, R. E.; Yazyev, O.; Austin, A. J.; Cammi, R.; Pomelli, C.; Ochterski, J. W.; Ayala, P. Y.; Morokuma, K.; Voth, G. A.; Salvador, P.; Dannenberg, J. J.; Zakrzewski, V. G.; Dapprich, S.; Daniels, A. D.; Strain, M. C.; Farkas, O.; Malick, D. K.; Rabuck, A. D.; Raghavachari, K.; Foresman, J. B.; Ortiz, J. V.; Cui, Q.; Baboul, A. G.; Clifford, S.; Cioslowski, J.; Stefanov, B. B.; Liu, G.; Liashenko, A.; Piskorz, P.; Komaromi, I.; Martin, R. L.; Fox, D. J.; Keith, T.; Al-Laham, M. A.; Peng, C. Y.; Nanayakkara, A.; Challacombe, M.; Gill, P. M. W.; Johnson, B.; Chen, W.; Wong, M. W.; Gonzalez, C.; Pople, J. A. *Gaussian 03*, Revision B. 02; Gaussian, Inc.: Pittsburgh, PA, 2003.
(23) Klamt, A.; Schürmann, G. *J. Chem. Soc., Perkin Trans. 2* **1993**, *2*, 799–805.
(24) Klamt, A. *J. Phys. Chem.* **1995**, *99*, 2224–2235.
(25) Eckert, F.; Klamt, A. *Aiche J.* **2002**, *48*, 369–385.
(26) Spek, A. L. *J. Appl. Crystallogr.* **2003**, *36*, 7−13.

NP900040W